Analyst

Accepted Manuscript

ROYAL SOCIETY OF CHEMISTRY

www.rsc.org/analyst

A comparative study of APLI and APCI in IMS at atmospheric pressure to reveal and explain peak broadening effects by the use of APLI.

Marvin Ihlenborg[1], Björn Raupers[1], Frank Gunzer[2] and Jürgen Grotemeyer[1,*]

1) Institute of Physical Chemistry, Christian-Albrechts-Universität zu Kiel, Max-Eyth-Str.1, 24118 Kiel

2) Physics Department, German University in Cairo, New Cairo City, Cairo Egypt

*Corresponding Author: Jürgen Grotemeyer, Institute of Physical Chemistry, Christian-Albrechts-Universität zu Kiel, Max-Eyth-Str.1, 24118 Kiel, +49 (0) 431 / 8807701, grote@phc.uni-kiel.de

ABSTRACT: The details of the ionization mechanism in atmospheric pressure are still not completely known. In order to obtain further insight into the occurring processes in atmospheric pressure laser ionization (APLI) a comparative study of atmospheric pressure chemical ionization (APCI) and APLI is presented in this paper. This study is carried out using similar experimental condition at atmospheric pressure employing a commercial ion mobility spectrometer (IMS). Two different peak broadening mechanisms can then be assigned, one related to a range of different species generated and detected, and furthermore for the first time a power broadening effect on the signals can be identified.

1. INTRODUCTION

APCI sources in atmospheric pressure ion mobility spectrometry (IMS) are common and widely used, e.g. in the detection of hazardous substances such as chemical warfare agents or explosives [1]. The ionization process is typically based on the proton transfer from protonated water clusters of different sizes (size depends on temperature and humidity level) to the analyte, consequently resulting in a protonated species [2]. Thus, the analyzed components need to have at least a higher proton affinity (PA) than the before-mentioned water clusters. At very low humidity levels, however, electron abstraction rather than protonation is observed to be the dominant ionization process [2].

For non-polar analytes it is possible to use an atmospheric pressure photo ionization (APPI) source in combination with an IMS [3, 4]. Typically, Krypton is used as a discharge gas to produce photons in the VUV range (10 eV or 124 nm respectively 10,6 eV or 117 nm). Ionization occurs via the production of a radical cation. The detected species are therefore this cation or, depending on the used solvent, proto-

nated species. A comparative study of APPI and APCI without using an IMS and direct detection with an Orbitrap mass spectrometer was recently published by Fredenhagen *et al.* [5].

Here a different approach will be followed by using a laser based ionization technique. Compared to a standard APPI source the wavelength tunability of laser systems allows a further improvement in the separation of an IMS as shown by Löhmannsröben *et al.* [6]. Like in Resonance enhanced Multi Photon Ionization (REMPI) [7] applied to mass spectrometry, a similar behavior in the ionization process can be observed in the IMS technique. If the laser wavelength coincides with an intermediate electronic state of a substance, a drastic increase of the signal intensity can easily be observed. Due to the photo physical processes underlying the multi photon ionization scheme, ions are generally formed with less internal energy than in other photo ionization techniques such as APPI.

First studies with this laser technique in conjunction with ion mobility spectrometry were conducted by D.M. Lubman and coworkers [8, 9] and later by G.A. Eiceman *et al.* [10]. Nowadays, this ionization technique is known as atmospheric pressure laser ionization APLI [11]. Both groups observed during their studies a stronger peak broadening by the use of APLI in comparison to similar studies with an APCI technique. While Lubman *et al.* attributed this observation to a longer drift length in the ionization region due to an exchange and introduction of a simple repeller in the APCI source, Eiceman and coworkers started to look in more detail at the effects of the laser during the ionization process. They concluded that an ion-ion repulsion during the ionization with APLI should cause this broadening behavior. However, a clear explanation of the broadening effect was not presented by either of them. Furthermore, in both experiments ambient pressure and elevated temperatures were used. Thus a direct conclusion for atmospheric pressure and room temperature is not appropriated.

We extended in this contribution these above mentioned investigations by a comparative study of the APCI and APLI with a commercial IMS at atmospheric pressure and room temperature. For APLI, no atmospheric pressure IMS is commercially available and therefore the measurements have to be carried out with a commercial setup as described in detail by Gunzer and coworkers [12]. The main goal is the validation the obtained signals, as well as a comparison concerning the differences obtained.

Since this is an initial study, the influence of only a few parameters has been investigated as well as the setup has not been optimized for the resolving power and other experimental parameters of minor interest. This is planned for future studies. But already here two unusual effects can be observed and a basic analysis regarding the cause of these effects will be described.

2. EXPERIMENTAL SECTION

A schematic view of the IMS 5000 (Dräger Safety GmbH & Co KG, Germany) used is shown in figure 1. Details for the different ionization methods are as follows: In both experiments a Dräger IMS 5000 Unit is used for the detection of the transferred ions; the detector unit at the end of the device is a stainless steel Faraday Cup with a diameter of 1 cm. All data are recorded with an oscilloscope of type LeCroy Waverunner 6051. Data processing is done with help of Origin (v 9.0, OriginLab Corporation). The software FITYK (v 0.9.8) [13] is used for the estimation of the resolving power for APCI.

Place figure 1 here.

All measurements are performed at atmospheric pressure and room temperature. Dry air with a water concentration lower than 90 ppbv is used as drift and sample gas. A mass flow controller (MFC) provides a constant drift gas flow (denoted $Q_{drift\ gas}$). Three further MFCs and corresponding parallel gas flows are used to control the sample gas flow (Q_{sample}). One gas flow was enriched with the analyte (here anisole and toluene) by passing the flow through a reservoir filled with the analyte ($MFC_{analyte}$), resulting in a saturated dry air flow with the analyte of a concentration around 200 ppmv for toluene and 20 ppmv for anisole. Afterwards, this flow was diluted to the desired concentration by adding another gas flow controlled by (MFC_{air}). Finally, this flow was combined with another flow containing water vapour saturated air (MFC_{water}). Thus, the final flow (Q_{sample}) contained the analyte in the desired concentration at the desired humidity level. A schematic view is given in figure 2. Red marks indicate components which have been removed for further experiments with toluene, where only dry air was used.

Place figure 2 here.

All chemicals were obtained from Sigma Aldrich and were used without further purification. The used water is deionized and produced in our laboratory.

2.1 APCI:

In brief, a ^{3}H-source (50 MBq, production year 2004) with 1 cm in diameter is placed 2 mm away from the grid, which separates the reaction region and drift region resulting in an ionization volume of 307.8 mm^{3}.

The control electronics are provided by a home built setup. Two high voltage power supplies (HCN 140-6500 respectively HCN 140-3500; FuG Elektronik GmbH, Germany) are used with a push/pull switch (HTS 41-06-GSM, Behlke Power Electronics GmbH, Germany) to obtain a time wise adjustable extraction pulse. The drift region is driven by a continuous electric field generated by a high voltage power supply (HCN 140-3500; also FuG Elektronik GmbH). The timing for the extraction pulse and the data acquisition is controlled by a delay generator (DG535, Stanford Research Systems, Inc., USA). The overall experimental frequency is 20 Hz.

The electric field strength of the extraction pulse accelerating the ions out of the reaction region is 1500 V/cm, the field strength in the drift region is 600 V cm^{-1}. APLI only provides positively charged ions and radical cations, the polarity of the fields has been set accordingly.

2.2 APLI:

For APLI measurements the ^{3}H source is exchanged by a simple pusher electrode. The details are also shown in figure 1. To couple a laser into the ionization region two windows are introduced in the apparatus. Due to the changes in the apparatus the point of ionization is 7 mm apart from the grid and the pusher 9 mm. The laser beam coupled perpendicular to the drift region of the IMS is of 2 mm in diameter resulting in an ionization volume of 44 mm^{3}.

For the REMPI experiments the fourth harmonic of an Nd:YAG Laser (operated at a frequency of 20 Hz, wavelength 266 nm; the laser is of type Surelite I, Continuum GmbH, Germany) is used. The Q-Switch delay of the laser is used for the timing of the experiment. For advanced experiments a positive lens (f = + 100 mm) is introduced into the beam in order to obtain a controllable focal point.

Due to the changes in the ionization technique and the use of a pulsed laser, some adjustments have to be made for the electronics. The potentials for the pusher electrode and the drift region are continuous and generated by two high voltage power supplies (HCN 140-6500 respectively HCN 140-3500; FuG Elektronik GmbH, Germany). A voltage of 4350 V is used for the pusher electrode and 3000 V for the drift region. Thus constant electric fields of 1500 V cm^{-1} are present in the ionization region and again 600 V cm^{-1} in the drift region.

3. RESULTS and DISCUSSION

For the first measurements anisole was used. Anisole has two important attributes that this study can benefit from. First, anisole has a higher PA (839.6 kJ/mol) compared to water (and clusters with one water molecule attached), thus it can be easily protonated under APCI conditions regarding protonation but also electron abstraction. Secondly, since an aromatic system is included in the structure, anisole can absorb light in the UV range with high efficiency and can therefore be used for APLI measurements. Thus it is an ideal substance for an initial comparison of both ionization techniques.

For APCI measurements first the reactant ion peak (RIP) was recorded. Afterwards, while keeping the gas flow and the relative humidity (rh) constant, the analyte was mixed with the gas flow. Because anisole has a higher PA than water clusters a clear change in the obtained spectrum can be observed (figure 3).

The drift time spectrum for anisole indicates two species with slightly different reduced mobilities (K_0) [14]. For all comparative measurements the used settings and obtained signal parameters are summarized in table 1. To get a first estimation of the resolving power two independent fit functions and additionally a Gaussian distribution for the diffusion were used (see figure 3b). Since two species are present, two different peak shapes have been combined with standard diffusion broadening, so that the experimental curve is reproduced (see for comparison the green and black curves in figure b). Thus, an averaged resolving power of $R_{exp,Anisole,APCI} = 37{,}3$ was obtained for APCI. This demonstrates the quality of the used commercial IMS and the method. Typical commercial setups achieve a resolving power of around 40.

Place figure 3 here

Place table 1 here

The obtained drift time spectra of anisole with APCI and APLI under similar experimental conditions are shown in figure 4. Two effects can clearly be recognized. The obtained signal for APLI increased in intensity and in the width of the peak compared to APCI. A resolving power of $R_{exp,Anisole,APLI} = 6{,}3$ is obtained. Thus the resolving power under same experimental conditions decreases about the 6-fold. It

should be noted that even at these signal intensities the detector system does not show any saturation (only at much stronger laser intensities signal saturation can be observed).

Place figure 4 here

Both effects are not expected. The number of detected ions, represented by the area under the curve (AUC), rises by ca. a factor of 11, while the ionization volume due to smaller dimensions of the laser beam decreases by a factor of seven. Thus APLI seems to have a higher ionization efficiency compared to APCI at least for polar aromatic systems. Furthermore, the usual negative effects regarding the resolving power, like unstable electric fields or turbulent flows [15], can be excluded as a cause for this effect because the same setup and experimental conditions were used for both measurements.

The unexpected strong peak broadening effect cannot be explained with the previous measurements published by Eiceman *et al.* or Lubman *et al.* [8-10] Furthermore, based on the principles published before [16], it would be assumed that a shorter extraction pulse length results in an increase in resolving power. Compared to the length of a laser pulse of 10 ns where ionization can take place to the extraction pulse length of 100 µs in APCI, the herein made observation can also not be explained.

Place figure 5 here

In order to get further insight, especially in light of these rather unexpected experimental results, we have used an additional method to explain the obtained peak broadening by the use of APLI; we have carried out a simulation based on the same experimental conditions. Focusing on the peak broadening, especially related to the ion cloud size produced by the laser pulse and its subsequent size increase due to diffusion and Coulomb repulsion, finite elements method calculations (FEM) and simulations have been performed. The FEM solver COMSOL [22] has been used for the development of the calculated ion cloud dimensions and related resolving powers can be seen in figure 5. These calculations starts with an initial ion cloud as large as the laser spot size of 100 μm^2.

Noteworthy to mention is the on purpose over estimation of the number of ions obtained by the ionization process. Reports in the literature [7, 8, 16] suggest an ion number of 10^9 ions per laser pulse, while

herein 10^{11} ions were estimated. Thus the coulomb interactions of the ions should have a higher impact on the peak broadening. The background of this approach is that the Coulomb interaction of the produced ions during APLI was mentioned earlier by Eicemann *et al.* as a possible explanation for the peak broadening by the use of APLI [10].

Even with the higher influence of the Coulomb interaction combined with the diffusion broadening a resolving power in this experiment should be far over 10 (i.e., much better than the one obtained in our experiments) and at least with the use of the same molecules the resolving power should not decrease when APLI is used.

The simulation also contradicts the explanation by Lubman *et al.* who stated that the decrease in resolving power is due to a longer drift length and to the changes in the ionization region [8]. The simulation clearly predicts a resolving power increase of the experiment with a longer drift time and therefore by the drift length of the IMS as expected from theory.

Place figure 6 here

Since literature and simulation cannot sufficiently explain the peak broadening under APLI conditions further investigations were carried out with toluene as a test molecule. Despite a further reduced resolving power, two main advantages can be designated for a further examination of the peak broadening effects.

The vacuum 0_0^0-transition is close to the used wavelength of the laser. Thus the ionization efficiency is further increased (see fig. 6). The intensity of the obtained signal is almost constant until a beam energy of the laser of about 150 µJ. Using lower laser energies the signal gets unstable. Furthermore, humidity has no significant influence on the signal intensity. In APCI measurements, humidity has a large influence on the signal intensity because it is directly involved in the ionization mechanism.

For APLI a slightly different gas flow system has been used. The MFC_{Water} was removed from the setup so that only dry air was used, i.e. no humidity added, and a larger analyte reservoir was used. The changes are marked red in figure 2.

3.1 Influence of the drift gas flow (fig. 7):

For a low drift gas flow (0 – 100 mL min^{-1}) a broad distribution of detected ions over a wide drift time range can be observed. Furthermore, a structure can be observed around the peak maxima. With increasing drift gas flow an increase in signal intensity in combination with a narrowing effect in the distribution of the drift time can be observed.

Place figure 7 here

Therefore it seems likely for APLI to generate unstable ion – molecule or fragment ion – molecule clusters in the ionization process which are then detected at the end of the drift region. A possible explanation for the supposed fragment ions could be an often observed ladder-switching mechanism [7, 18].

Due to an increase in collisions by increasing the drift gas flow it is possible for the unstable clusters to fragment and thus to result in only one stable detected ion or ion – molecule cluster [19, 20].

3.2 Influence of the laser energy (fig. 8):

To study the influence of the laser energy the laser beam was focused with a biconvex lens directly in the ionization region. Initially, the obtained spectra seem to increase in intensity with increasing laser energy. A detailed analysis of the peak intensities and shapes, however, reveals a different behavior for the intensity and the peak width.

While the intensity of the peaks reaches a maximum at a laser energy around 200 µJ and decreases afterwards, the FWHM and the detected ions (represented by the AUC) rises further up to an energy around 400 µJ and remains then constant with increasing laser energies. It is interesting to observe that the increase in FWHM is driven by the broadening of the tailing while the peak maximum does not change in drift time. Thus our measurements do not show the same behavior as those of Eiceman *et al.* [10]. Their dependence of the signal intensity on the laser power was a monotonous one over the same energy range as the one investigated here (pulse energies between 250 µJ and 1000 µJ). Our results show an increase, but also a decrease after the maximum at 200 µJ. The behavior of the peak width was not investigated by Eiceman and coworkers [10]. However, additional effects are active in the data presented in our measurements, especially in addition to the expected Coulomb repulsion, which require further investigations. Such a discrimination of the peak intensity while the peak width and the peak area remains constant is known in spectroscopy as power broadening [21]. A comparable observation of

this behavior in IMS does not exist to our knowledge. Therefore, for the first time, a power broadening effect in atmospheric pressure IMS at room temperature with an APLI is observed. On base of the data shown above further investigations are necessary to reveal the details of the causing effects. It is obvious that the ion – ion repulsion of the analyte seem not to be solely responsible for this effect. We conclude this fact because the AUC remains the same after 400 µJ of laser energy. This value should also increase further since the higher laser energies should lead to more ions being produced. Therefore, a higher ion concentration resulting in a peak broadening by ion - ion repulsion should not cause the observed behavior as stated out in earlier an interpretation [10].

Place figure 8 here

4. CONCLUSION

In this study we have shown spectra of a comparative study for APLI and APCI with anisole and toluene to reveal a strong peak broadening effect for the use of APLI in atmospheric pressure IMS. We were not able to explain this observation with common effects, like diffusion broadening, concentration effects leading to ion-ion repulsion or changes in the ionization/reaction region, in IMS at atmospheric pressure.

However, at this point we are able to explain this effect by two observations. Additional aspects cannot be ruled out at this stage of investigation. Firstly, due to the influence of the variation of laser energy on the peak area, the spectra seem to indicate that power broadening mechanisms play an important role which have not been described for such an experiment before. Further investigations on this behalf and on the wavelength dependency have to be made.

A second effect can also be assigned to the peak broadening effect. A wide range of unstable ions, fragments and clusters can be detected for low drift gas flows. Thus a simple comparison to a direct APCI, APPI and APLI coupled to mass spectrometers is not possible and further experiments have to be made.

5. ACKNOWLEDGMENT

The support by the Deutsche Forschungsgemeinschaft (DFG Grant Gr 917-33-1) is gratefully acknowledged.

REFERENCES

[1] M.A. Mäkinen, O.A. Anttalainen, M.E.T. Sillanpää, "Ion Mobility Spectrometry and Its Applications in Detection of Chemical Warfare Agents", Anal. Chem. 82 (2010) 9594-9600; doi: http://dx.doi.org/10.1021/ac100931n.

[2] G.A. Eiceman, Z. Karpas, "Ion Mobility Spectrometry", second ed., CRC Press, Boca Raton, 2005.

[3] H. Borsdorf, E. Nazarov, R. Miller, "Atmospheric-pressure ionization studies and field dependence of ion mobilities of isomeric hydrocarbons using a miniature differential mobility spectrometer", Anal. Chim. Acta 575 (2006) 76-88; doi: http://dx.doi.org/10.1016/j.aca.2006.05.066.

[4] J. Laakia, A. Adamov, M. Jussila, C.S. Pedersen, A.A. Sysoev, T. Kotiaho, "Separation of Different Ion Structures in Atmospheric Pressure Photoionization-Ion Mobility Spectrometry-Mass Spectrometry (APPI-IMS-MS)", J Am So Mass Spectrom 21 (2010) 1565-572; doi: http://dx.doi.org/10.1016/j.jasms.2010.04.018.

[5] A. Fredenhagen, J. Kühnöl, "Evaluation of the optimization space for atmospheric pressure photoionization (APPI) in comparison with APCI", J. Mass Spectrom. 2014, 49, 727-736; doi: http://dx.doi.org/10.1002/jms.3401.

[6] H.-G. Löhmannsröben, T. Beitz, "Laser-based ion mobility spectrometry for sensing of aromatic compounds", Postprints der Universität Potsdam: Mathematisch-Naturwissenschaftliche Reihe 2007, 3; doi: http://dx.doi.org/10.1117/12.559509.

[7] J. Grotemeyer, E.W. Schlag, "Multiphoton-Ionisations-Massenspektrometrie;ein neues Hilfsmittel in der Analytik." Angew.Chem., **100**, 461-474 (1988), doi: http://dx.doi.org/10.1002/ange.19881000404.

[8] D.M. Lubman, M.N. Kronick, "Plasma Chromatography with Laser-Produced Ions", Anal. Chem. 54 (1982) 1546-1551; doi: http://dx.doi.org/10.1021/ac00246a021.

[9] D.M. Lubman, M.N. Kronick, "Discrimination of Isomers of Xylene by Resonance Enhanced Two-Photon Ionization", Anal. Chem. 54 (1982) 2289-2291; doi: http://dx.doi.org/10.1021/ac00250a033.

[10] G.A. Eiceman, V.J. Vandiver, C.S. Leasure, G.K. Anderson, J.J. Tiee, W.C. Danen, "Effects of Laser Beam Parameters in Laser Ion Mobility Spectrometry", Anal. Chem. 58 (1986) 1690-1695; doi: http://dx.doi.org/10.1021/ac00121a020.

[11] M. Constapel, M. Schellenträger, T. Benter, "Atmospheric-pressure laser ionization: a novel ionization method for liquid chromatography/mass spectrometry", Rapid Commun. Mass Spectrom. 19 (2005) 326-336; doi: http://dx.doi.org/10.1002/rcm.1789.

[12] F. Gunzer, S. Zimmermann, W Baether, "Application of a Nonradioactive Pulsed Electron Source for Ion Mobility Spectrometry", Anal. Chem. 82 (2010) 3756–3763; doi: http://dx.doi.org/10.1021/ac100166m.

[13] M. Wojdyr, "Fityk: a general-purpose peak fitting program", J. Appl. Crys. 43 (2010) 1126-1128; doi: doi:10.1107/S0021889810030499

[14] G.E. Spangler, "Expanded theory for the resolving power of a linear ion mobility spectrometer", International Journal of Mass Spectrometry 220 (2002) 399-418; doi: http://dx.doi.org/10.1016/S1387-3806(02)00841-2.

[15] P. Watts, A. Wilders, "On the resolution obtainable in practical ion mobility systems", International Journal of Mass Spectrometry and Ion Processes 112 (1992) 179-190; doi: http://dx.doi.org/10.1016/0168-1176(92)800.

[16] A.B. Kanu, M.M. Gribb, H.H. Hill, "Predicting Optimal Resolving Power for Ambient Pressure Ion Mobility Spectrometry", Anal. Chem. 80 (2008) 6610-6619; doi: http://dx.doi.org/10.1021/ac8008143.

[17] J.P. Reilly, K.L. Kompa, "Laser induced multiphoton ionization mass spectrum of benzene", J. Chem. Phys. 73 (1980) 5468-5476; doi: http://dx.doi.org/10.1063/1.440092.

[18] U. Boesl, H.J. Neusser, E.W. Schlag, "Visible and UV multiphoton ionization and fragmentation of polyatomic molecules", *J. Chem. Phys. 72 (*1980) 4327-4333; doi: http://dx.doi.org/10.1063/1.439712.

[19] A.W. Castleman, R.G. Keesee, "Ionic Clusters", Chem. Rev. 86 (1986) 589-618; doi: http://dx.doi.org/10.1021/cr00073a005.

[20] A.P. Bruins, "Mass spectrometry with ion sources operating at atmospheric pressure", Mass Spectrometry Reviews. 10 (1991) 53-77; doi: http://dx.doi.org/10.1002/mas.1280100104.

[21] N. Vitanov, B. Shore, L. Yatsenko, K. Bähmer, T. Halfmann, T. Rickes, K. Bergmann, "Power broadening revisited: theory and experiment", Optics Communications 2001, 199, 117-126; doi: http://dx.doi.org/10.1016/S0030-4018(01)01495-X.

[22] COMSOL Multiphysics v. 4.3B, www.comsol.com.

Table 1: Overview of experimental parameters and resulting experimental values for the comparison of the drift time spectra with APLI and APCI.

	Anisole		**Toluene**
	APCI	*APLI*	*APLI*
$Q_{drift\ gas}$ [mL min^{-1}]	15	15	15
Q_{sample} [mL min^{-1}]	20	20	20
Q_{water} [mL min^{-1}]	20	20	20
Q_{air} [mL min^{-1}]	20	20	20
$E_{ionisation\ region}$ [V]	3300	4350	4350
$E_{drift\ region}$ [V]	3000	3000	3000
$t_{Ionisation}$ [µs]	100	0,01	0,01
E_{laser} [µJ]		850	700
t_{max} [ms]	7,87	7,55	7,62
	8,06		
K_0 [$cm^2\ V^{-1}\ s^{-1}$]	0,98	1,03	1,02
	0,96		
FWHM [ms]	0,269	1,19	1,64
	0,199		
R	34,1	6,3	3,9
	40,5		
AUC [a.u.]	4,487	48,09	190,6

Figure Captions

Figure 1. Experimental Setup. Sketch of the used Dräger IMS 5000 with the APCI source and the used timing is shown in the upper right part. Modifications and the APLI source are shown in the lower part of the figure. The laser beam is irriaditated perpenticular to the drift region into the IMS.

Figure 2. Used gas flow system. Marked in red are components which have been removed for further APLI measurements with toluene.

Figure 3. A) Drift time spectrum of anisole with APCI. Experimental data can be found in table 1. B) Enlargement of the experimental signal and a data interpretation with FITYK.

Figure 4. Drift time spectra of anisole comparing APCI and APLI. For both spectra the same experimental options have been chosen and can be found in table 1.

Figure 5. Simulated FWHM with rising drift times and the corresponding resolving power.

Figure 6. Drift time spectra of anisole and toluene at different laser energies and for toluene without water in the sample gas flow. All other experimental conditions can be found in table 1.

Figure 7. Variation of the drift gas flow with Q_{sample} = 60 mL min^{-1} (17% analyte), t_{laser} = 10 ns, λ_{Laser} = 266 nm, $ø_{Laser}$ = 1 mm; E_{Laser} < 70 µJ; V_{Pusher} = 4350 V and V_{Drift} = 3000 V.

Figure 8. Variation of the laser energy with a focus into the ion region. Q_{sample} = 60 mL min^{-1} (17% analyte), $Q_{drift\ gas}$ = 950 mL min^{-1}, t_{laser} = 10 ns, λ_{Laser} = 266 nm, $ø_{Laser}$ = 2 mm, f = + 100 mm, V_{Pusher} = 4350 kV and V_{Drift} = 3000 V.

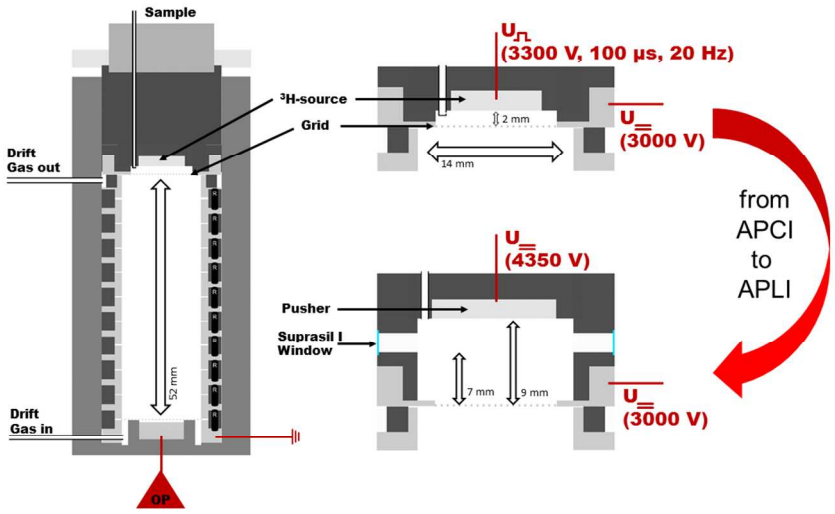

Figure 1. Experimental Setup. Sketch of the used Dräger IMS 5000 with the APCI source and the used timing is shown in the upper right part. Modifications and the APLI source are shown in the lower part of the figure. The laser beam is irriaditated perpenticular to the drift region into the IMS.
338x190mm (96 x 96 DPI)

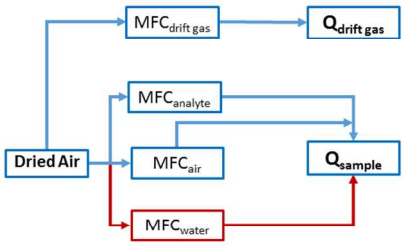

Figure 2. Used gas flow system. Marked in red are components which have been removed for further APLI measurements with toluene.
338x190mm (96 x 96 DPI)

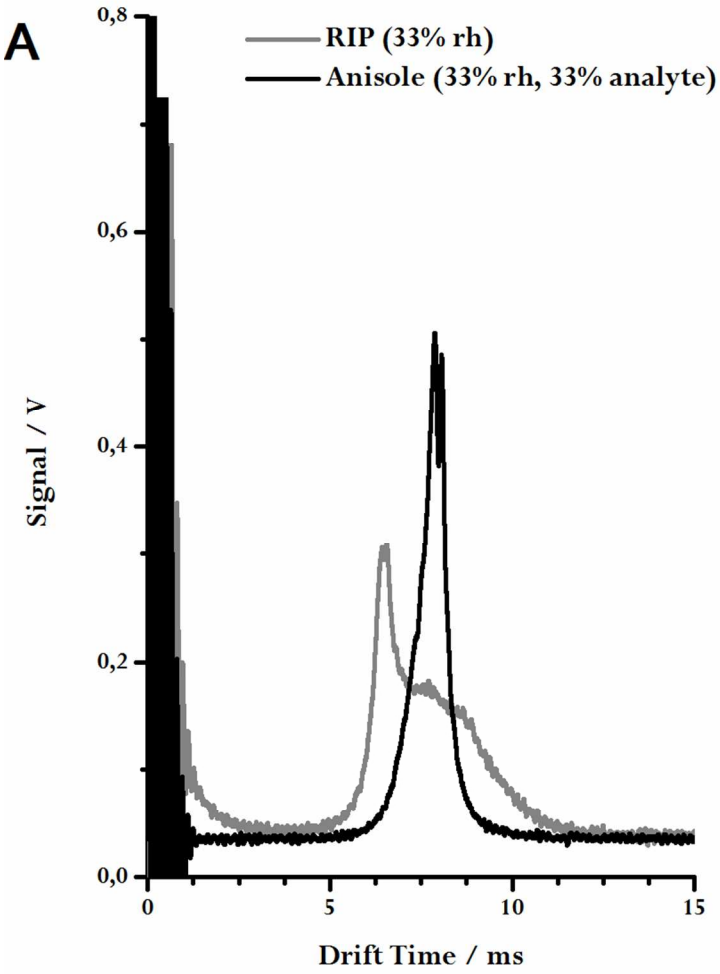

Figure 3. A) Drift time spectrum of anisole with APCI. Experimental data can be found in table 1. B) Enlargement of the experimental signal and a data interpretation with FITYK.
76x114mm (300 x 300 DPI)

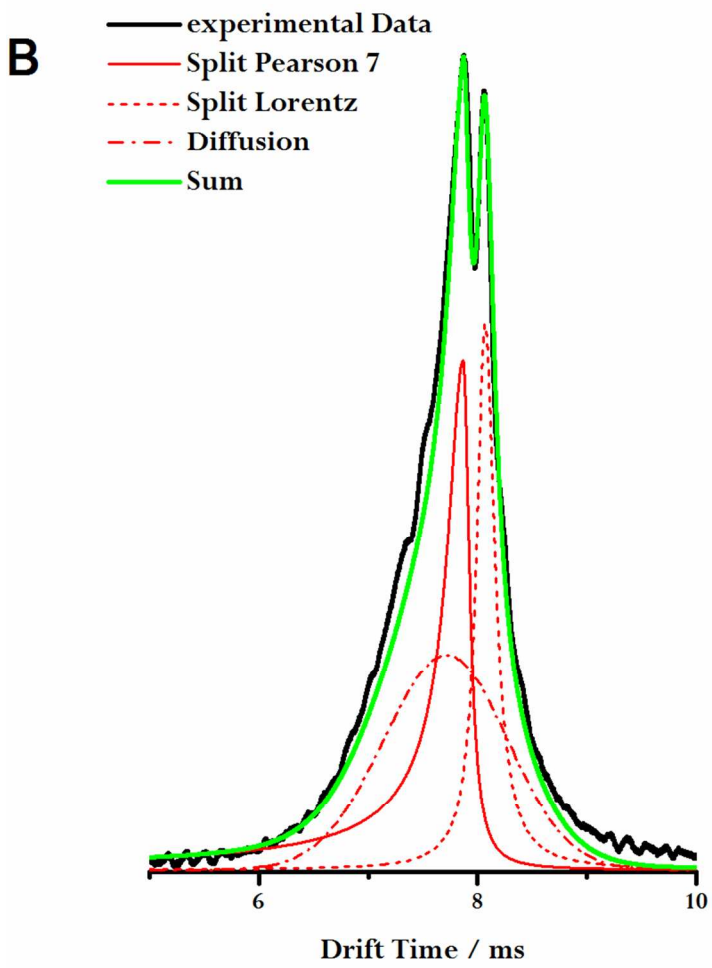

Figure 3. A) Drift time spectrum of anisole with APCI. Experimental data can be found in table 1. B) Enlargement of the experimental signal and a data interpretation with FITYK.
76x114mm (300 x 300 DPI)

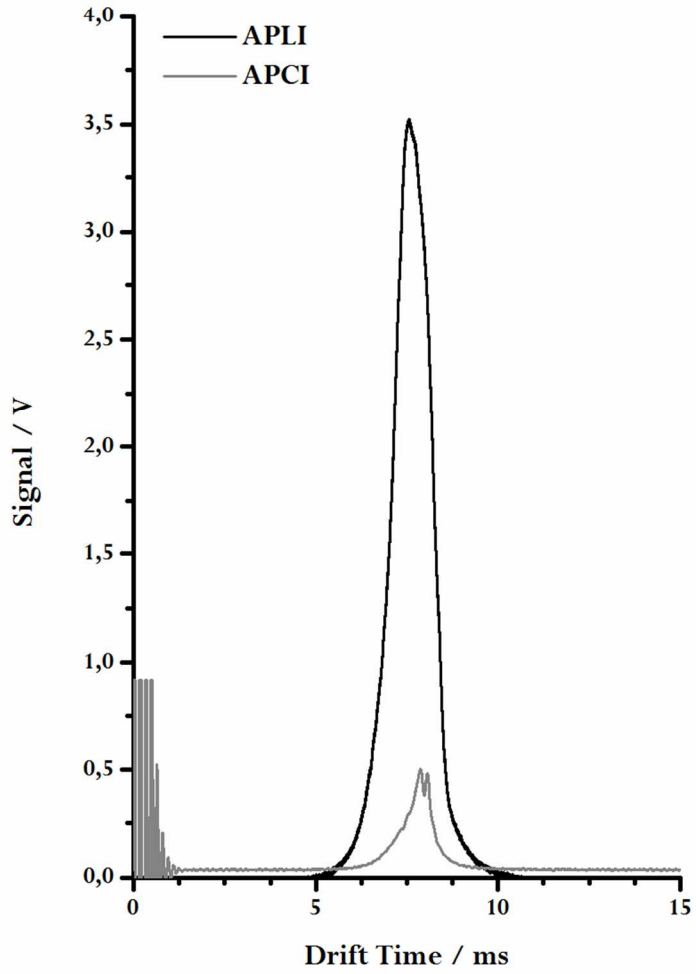

Figure 4. Drift time spectra of anisole comparing APCI and APLI. For both spectra the same experi-mental options have been chosen and can be found in table 1.
76x114mm (300 x 300 DPI)

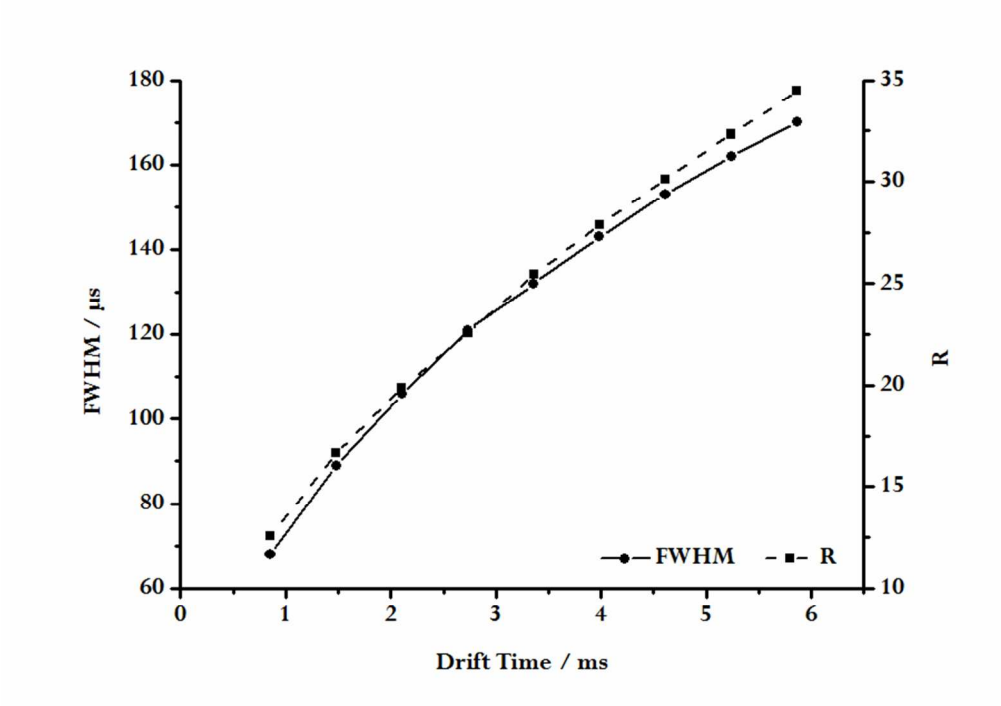

Figure 5. Simulated FWHM with rising drift times and the corresponding resolving power.
76x53mm (300 x 300 DPI)

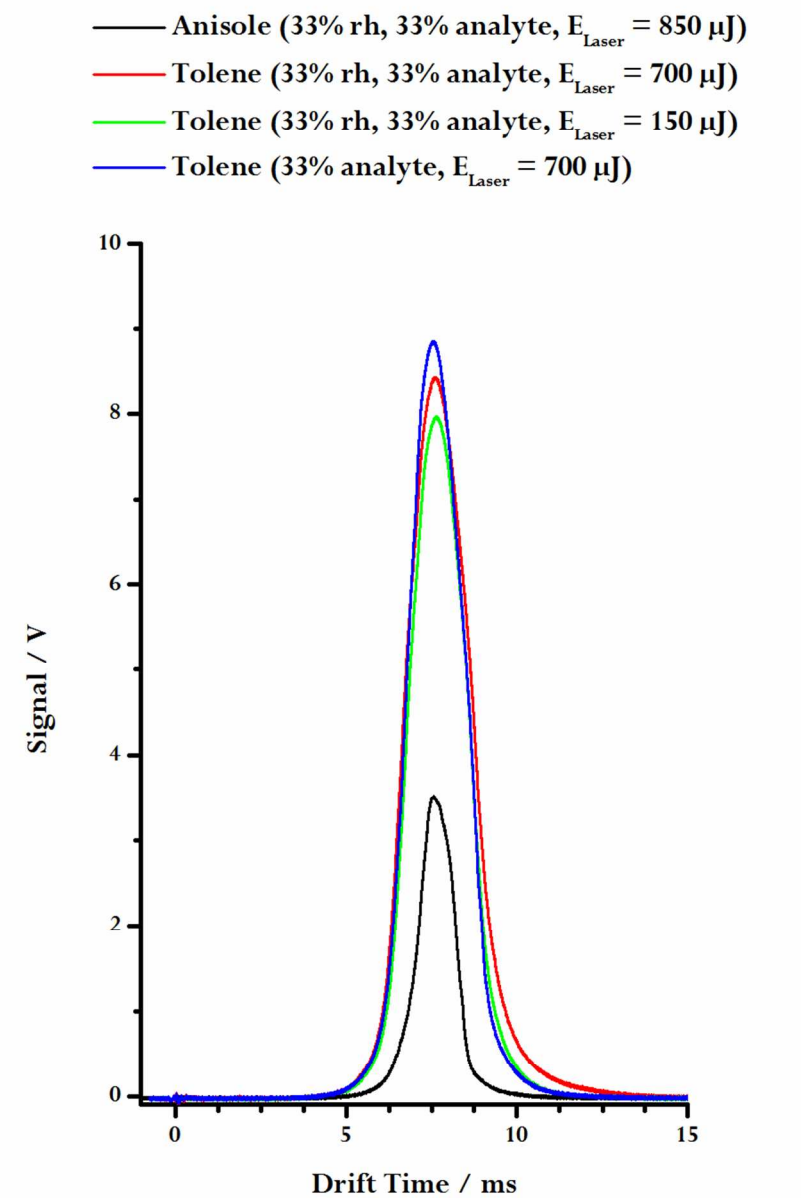

Figure 6. Drift time spectra of anisole and toluene at different laser energies and for toluene without water in the sample gas flow. All other experimental conditions can be found in table 1.
76x114mm (300 x 300 DPI)

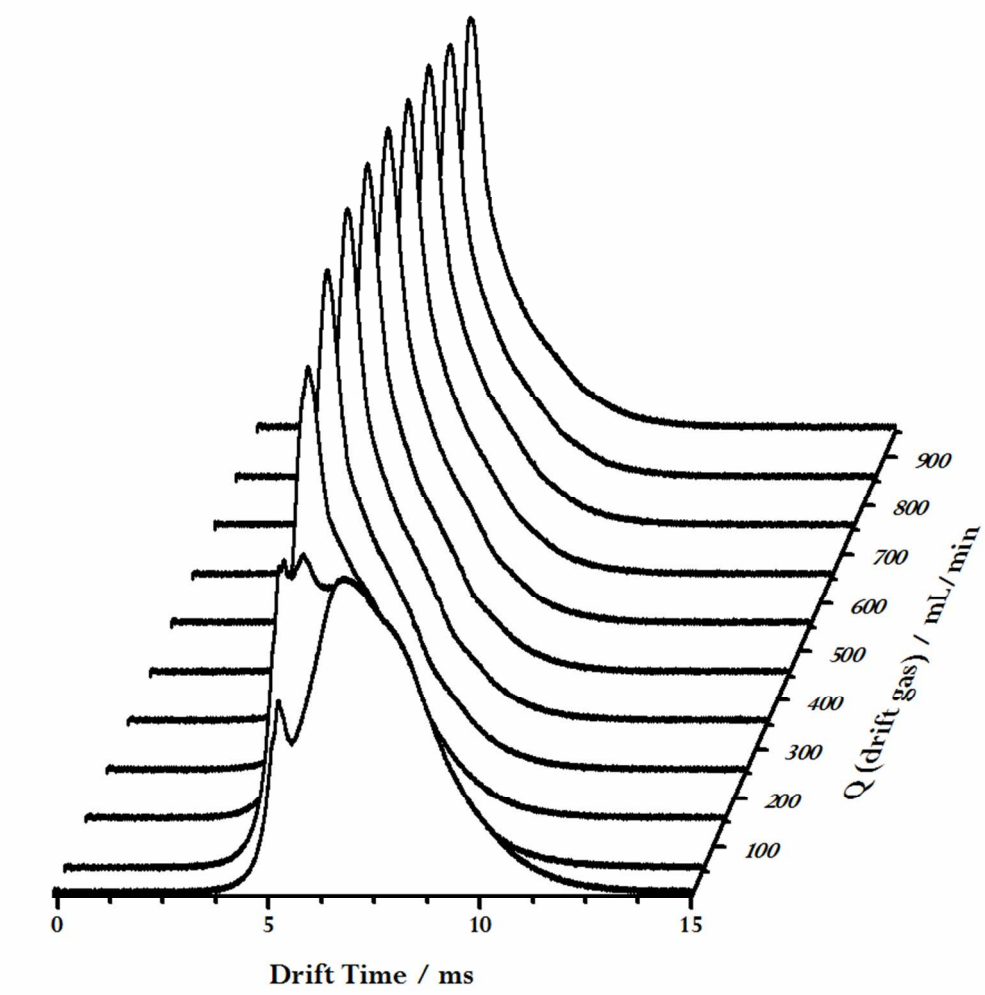

Figure 7. Variation of the drift gas flow with Qsample = 60 mL min-1 (17% analyte), tlaser = 10 ns, λLa-ser = 266 nm, øLaser = 1 mm; ELaser < 70 µJ; VPusher = 4350 V and VDrift = 3000 V.
76x76mm (300 x 300 DPI)

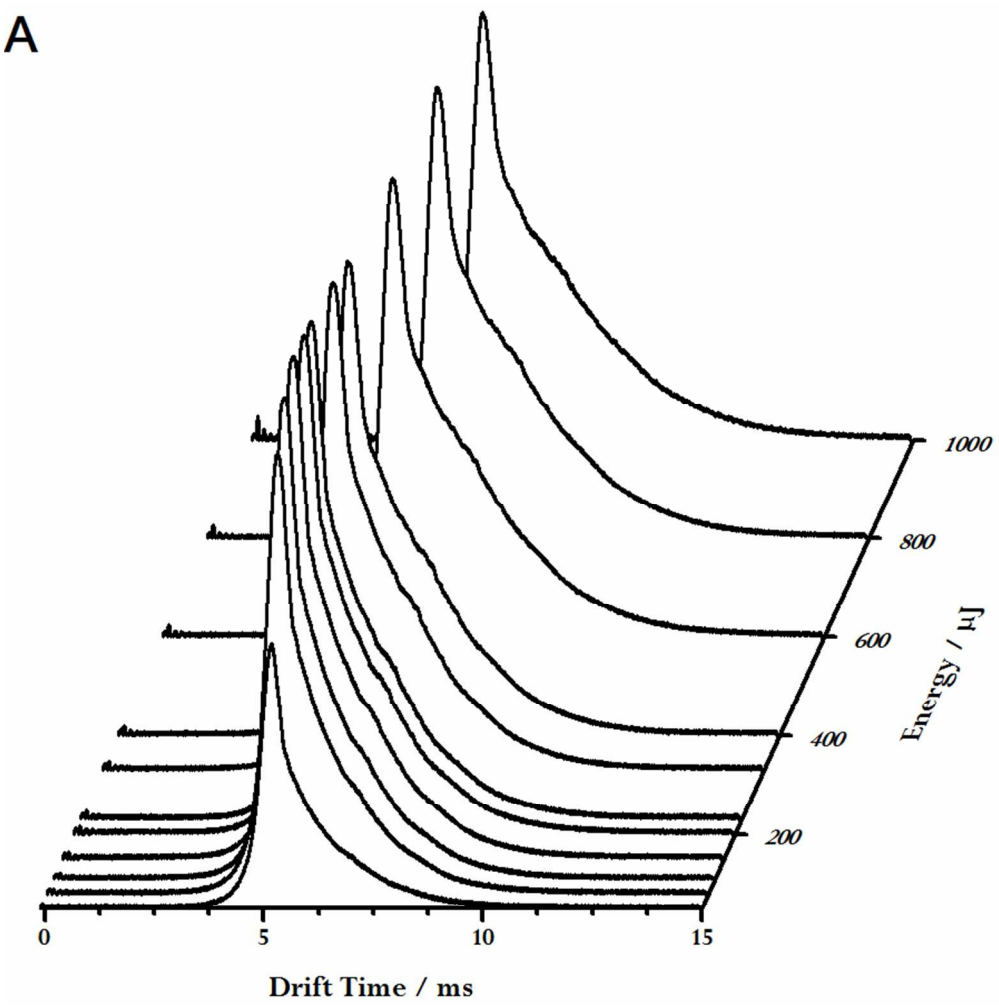

Figure 8. Variation of the laser energy with a focus into the ion region. Qsample = 60 mL min-1 (17% analyte), Qdrift gas = 950 mL min-1, tlaser = 10 ns, λLaser = 266 nm, øLaser = 2 mm, f = + 100 mm, VPusher = 4350 kV and VDrift = 3000 V.
76x76mm (300 x 300 DPI)

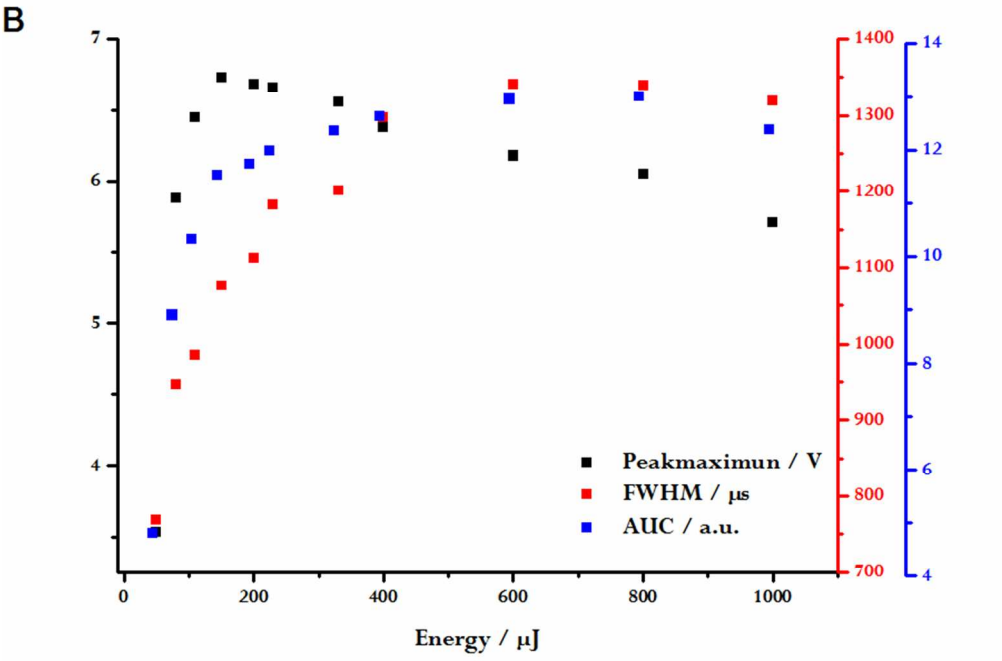

Figure 8. Variation of the laser energy with a focus into the ion region. Qsample = 60 mL min-1 (17% analyte), Qdrift gas = 950 mL min-1, tlaser = 10 ns, λLaser = 266 nm, øLaser = 2 mm, f = + 100 mm, VPusher = 4350 kV and VDrift = 3000 V.
76x50mm (300 x 300 DPI)